Amplified subtropical stationary waves in boreal summer and their implications for regional water extremes

This content has been downloaded from IOPscience. Please scroll down to see the full text.

2015 Environ. Res. Lett. 10 104009

(http://iopscience.iop.org/1748-9326/10/10/104009)

View the table of contents for this issue, or go to the journal homepage for more

Download details:

IP Address: 210.77.64.105
This content was downloaded on 13/04/2017 at 10:21

Please note that terms and conditions apply.

You may also be interested in:

Possible causes of the Central Equatorial African long-term drought
Wenjian Hua, Liming Zhou, Haishan Chen et al.

Recent interdecadal changes in the interannual variability of precipitation and atmospheric circulation over northern Eurasia
Tetsuya Hiyama, Hatsuki Fujinami, Hironari Kanamori et al.

Projected changes in regional climate extremes arising from Arctic sea ice loss
James A Screen, Clara Deser and Lantao Sun

Teleconnections associated with the intensification of the Australian monsoon during El Niño Modoki events
A S Taschetto, R J Haarsma, A Sen Gupta et al.

Influence of the Gulf Stream on the Barents Sea ice retreat and Eurasian coldness during early winter
Kazutoshi Sato, Jun Inoue and Masahiro Watanabe

How does the SST variability over the western North Atlantic Ocean control Arctic warming over the Barents–Kara Seas?
Ok Jung, Mi-Kyung Sung, Kazutoshi Sato et al.

On the decreasing trend of the number of monsoon depressions in the Bay of Bengal
S Vishnu, P A Francis, S S C Shenoi et al.

Evidence for a wavier jet stream in response to rapid Arctic warming
Jennifer A Francis and Stephen J Vavrus

IOP Publishing Environ. Res. Lett. 10 (2015) 104009 doi:10.1088/1748-9326/10/10/104009

Environmental Research Letters

RECEIVED
20 July 2015

REVISED
9 September 2015

ACCEPTED FOR PUBLICATION
18 September 2015

PUBLISHED
14 October 2015

LETTER

Amplified subtropical stationary waves in boreal summer and their implications for regional water extremes

Jiacan Yuan[1], **Wenhong Li**[1] and **Yi Deng**[2]

[1] Division of Earth and Oceanic Sciences, Nicholas School of the Environment, Duke University, Durham, NC, USA
[2] School of Earth and Atmospheric Sciences, Georgia Institute of Technology, Atlanta, GA, USA

E-mail: wenhong.li@duke.edu

Keywords: subtropical stationary waves, moisture flux, weather extremes, drought, heavy rainfall, precipitation

Abstract

The linkage between climate change and increased frequency/magnitude of weather extremes remains an open question in the scientific field. Here we investigate such a dynamical linkage by focusing on an amplification trend of the northern subtropical stationary waves found in recent decades. Specifically, we show that in multiple modern reanalysis products, a robust positive trend exists in a wave amplitude index defined through the summer-mean tropospheric stream function field. Pronounced changes in the subtropical atmospheric circulation accompany this wave amplification, including an intensified South Asian monsoon and strengthened subtropical highs over the North Pacific and North Atlantic oceans. Through modifying the characteristics of large-scale moisture transport, these circulation changes are coupled to changes in the regional precipitation amount and the occurrence of water extremes including both droughts and heavy rainfall events. Given this connection, amplified stationary waves have likely contributed to the elevated occurrence probabilities of droughts in the central United States, Mexico, Japan, and northern China, as well as those of heavy rainfall events in South Asia, southeastern China, and the eastern United States. These results suggest that as climate warming continues, the amplification of subtropical stationary waves will increase the risk of water extremes over the above-mentioned regions.

1. Introduction

In recent decades, a large number of weather extremes have been observed in the northern hemisphere (NH) (Min *et al* 2011, Rahmstorf and Coumou 2011, Dole *et al* 2011, Coumou and Rahmstorf 2012, Coumou *et al* 2013). What causes the increased frequency of weather extremes in the warming climate is an important question, which has raised broad interest in both scientific and socioeconomic fields (Min *et al* 2011, Pall *et al* 2011, Rahmstorf and Coumou 2011, Screen and Simmonds 2014). Many recent studies have suggested that the amplification of planetary waves represents a dynamical linkage between weather extremes and long-term climate change (Francis and Vavrus 2012, 2015, Liu *et al* 2012, Petoukhov *et al* 2013, Coumou *et al* 2014). Most of these studies concentrate on the impact of Arctic amplification (Screen and Simmonds 2010)—rapid surface warming over the Arctic—which is an important feature of climate change. It has been proposed that high-amplitude planetary waves due to the Arctic amplification could favor persistent weather patterns, which may increase the probabilities of weather extremes (Francis and Vavrus 2012, 2015, Petoukhov *et al* 2013, Coumou *et al* 2014, Tang *et al* 2014). There is an ongoing debate about observational and modeling evidence for this hypothesis in the scientific community (Barnes 2013, Hassanzadeh *et al* 2014, Screen and Simmonds 2013, Woollings *et al* 2014). During the NH summer, the Arctic amplification is at the weakest annually, especially in the subtropics (Screen and Simmonds 2010). Is there any other process by which planetary waves could link the water extremes (i.e. drought and heavy-rainfall events) to the warming climate, besides the aforementioned hypotheses that evoke Arctic amplification?

In the boreal summer, weather and climate in the subtropics are governed by subtropical high-pressure systems (Davis *et al* 1997, Rodwell and Hoskins 2001, Miyasaka and Nakamura 2005, Li *et al* 2011) and monsoon low-pressure systems (Holton 1992, Chen 2003, Adams and Comrie 1997) in the lower atmosphere, which are well portrayed by subtropical stationary waves (Nigam and DeWeaver 2003, Chen 2010). In this study, we focus on the zonal band 15 °N–45 °N, to cover the area of the subtropical highs and monsoon lows. Generally speaking, NH stationary waves, which are due to zonally asymmetric orography and land–sea thermal contrast, are planetary waves with phase speed close to zero (Chen and Trenberth 1988, Hoskins and Karoly 1981, Nigam and DeWeaver 2003). Ting (1994) demonstrated that global diabatic heating plays an important role in maintaining the subtropical stationary waves in summer.

The intensification of land–sea thermal contrast since the 1950s, which was observed in previous studies (Braganza *et al* 2004, Kamae *et al* 2014), is an important response to climate warming (Braganza *et al* 2004, Sutton *et al* 2007, Li *et al* 2012, 2013), and the maximum land–sea temperature ratio is found in the subtropics (Sutton *et al* 2007). Since subtropical stationary waves largely depend on diabatic heating, which is closely related to land–sea thermal contrast, it raises the question of how the stationary waves change in the context of enhanced land–sea thermal contrast. However, most of the previous research investigated regional changes in subtropical circulation, with subtropical highs and monsoon lows treated *separately*. Both observational evidence and model simulations show that marine subtropical high-pressure systems have become stronger in recent decades (Sui *et al* 2007, Zhou *et al* 2009, Li *et al* 2011, 2012), and the NH summer monsoon has intensified in the last three decades (Wang *et al* 2012, 2013). The overall amplitude changes in subtropical stationary waves over the hemispheric domain have not been investigated before. Studying the subtropical stationary waves could identify a coherent change and the overriding controls on the hemispheric scale. In addition, the moisture transport by large-scale flows associated with stationary waves contributes generally to regional hydroclimate variability (Nigam and DeWeaver 2003), but the implication of changes in subtropical stationary waves on regional water *extremes* remains unclear.

This study investigates the change in subtropical stationary wave amplitude in the boreal summer. Specific questions addressed in this study are: (1) have the northern subtropical stationary waves amplified during recent decades? (2) How might changes in the stationary-wave amplitude contribute to regional precipitation amounts and water extremes? Results from this study will improve our understanding of the dynamical link between global warming and changes in water extremes in the boreal summer. Since roughly 63% of the world’s population lives in the zonal band 15 °N–45 °N (based on ISLSCP II Global Population of the World (Balk *et al* 2010)), this study is important for assessing the socioeconomic impacts of climate change.

2. Data and methods

In this study, stream function and moisture flux are derived from horizontal winds and specific humidity from the European Center for Medium-Range Weather Forecasts (ECMWF) ERA-Interim reanalysis data (Dee *et al* 2011) on a 1.5° × 1.5° latitude–longitude grid. We analyse the boreal summer (June, July, and August) from 1979 to 2013. The precipitation is derived from the Climate Prediction Center (CPC) unified gauge-based analysis of global daily precipitation (Chen *et al* 2008) with a resolution of 0.5° × 0.5°.

We denote the zonal amplitude of subtropical stationary waves by the variance of the stream function at 30 °N, which measures the intensity of the atmospheric troughs and ridges in the NH subtropics. This is motivated by the climatology of the eddy stream function in the boreal summer at 925 hPa (figure 1(a)) and 300 hPa (figure 1(b)), in which the centers of the stationary waves are located at approximately 30 °N. To facilitate the quantification of features associated with the change in stationary wave amplitude, we define a stationary wave index (SWI) as the zonal variance of the 925 hPa stream function at 30 °N. We perform this calculation on the seasonal mean data for each summer season. The results of positive trends are not sensitive to the precise choice of latitude within the latitude band between 25 °N and 35 °N or pressure levels in the lower troposphere for defining the SWI (not shown). We focus on the lower level troposphere to study the changes in stationary wave amplitude and their implications on water extremes because most water vapor is confined to the lower levels (Holloway and Neelin 2009). We categorize strong (weak) SWI years as those years in which the SWI exceeded its mean plus (minus) one standard deviation. Strong (weak) SWI years indicate that the amplitude of the subtropical stationary wave is relatively large (small). Based on this criterion, we obtain 7 strong SWI years: 1990, 1994, 2002, 2010, 2011, 2012 and 2013, and 7 weak SWI years: 1979, 1981, 1987, 1992, 1993, 1995 and 1996.

To study water extremes, we use heavy-rainfall days and dry days. A heavy-rainfall day is defined as a day on which the precipitation exceeds the 95th percentile of daily precipitation over the whole time period. We choose the 95th percentile cutoff as the criterion so that the threshold is rare enough to be considered extreme but not so rare as to severely limit the number of cases. A dry day is defined as a day without precipitation. At each spatial grid point, we count the number of heavy-rainfall and dry days in every summer from 1979 to 2013.

Since some variables do not follow the normal distribution (e.g. precipitation, number of extreme days),

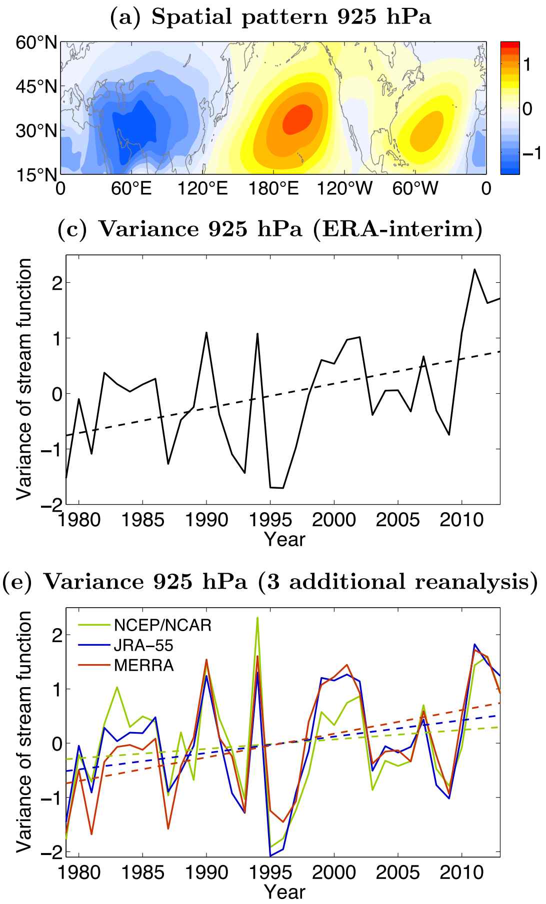

Figure 1. Climatology of eddy stream function at (a) 925 hPa and (b) 300 hPa in JJA during 1979–2013 (unit: 10^7 m^2 s^{-1}) with ERA-interim reanalysis data. Warm colors in (a) and (b) denote anti-cyclonic circulation, and cool colors cyclonic circulation. Normalized variance of eddy stream function at 30 °N in JJA at (c) 925 hPa and (d) 300 hPa with ERA-interim reanalysis data. (e) Same as (c) except for 3 additional reanalysis data points: NCEP/NCAR, JRA-55 and MERRA. The dashed lines denote the linear trends obtained by the least squares method.

we use a Monte Carlo method to test the statistical significance. For instance, when we calculate the statistical significance of the difference between composites based on the strong and weak SWI years, we randomly choose 14 years from 1979 to 2013. These 14 years are divided into 2 groups (7 years in each group). We composite values of a particular field based on each group and then calculate the difference of the composite between these two groups. We repeat this process 1000 times and obtain an empirical distribution at each grid point. If the difference between the actual composite based on strong and weak SWI years exceeds the 95th percentile or is less than the 5th percentile of the empirical distribution, we claim the difference is statistically significant at the 90% level at that grid point.

3. Results

3.1. Changes in the stationary wave amplitude in the boreal summer

The spatial patterns of climatological stationary waves in the lower (925 hPa) and upper (300 hPa) troposphere are shown in figures 1(a) and (b), respectively. Consistent with previous studies (Chen 2010, White 1982), the subtropical stationary waves are vertically anti-phased in the subtropics. Over the oceans, two anticyclones at the lower level are underneath the upper level cyclones. These are the North Pacific Subtropical High (NPSH) (Sui *et al* 2007) and the North Atlantic Subtropical High (NASH) (Davis *et al* 1997, Li *et al* 2011). Also, a continental-scale cyclone appears over Eurasia (White 1982, Chen 2003) and a weak cyclone is present over the southwestern United States and Mexico (Adams and Comrie 1997). These are essential parts of the Asian Monsoon circulation and the North American Monsoon circulation, respectively (Nigam and DeWeaver 2003).

From 1979 to 2013, the zonal variance of the 30 °N stream function exhibits an upward trend at both 925 hPa (figure 1(c)) and 300 hPa (figure 1(d)). The rate of increase is 2.02×10^{11} m^4 s^{-2} per year for 925 hPa and 1.02×10^{11} m^4 s^{-2} per year for 300 hPa. The trend of the variance at 925 hPa is statistically significant at the 95% level based on the Mann–Kendall test. We also calculate the SWI with three additional reanalysis data sets: MERRA reanalysis data (Rienecker *et al* 2011) from the National Aeronautics and

(a) Climatology

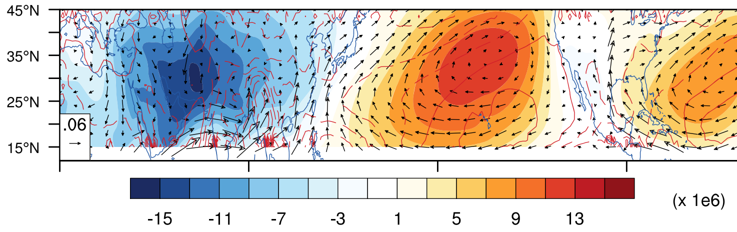

(b) Strong SWI years composite

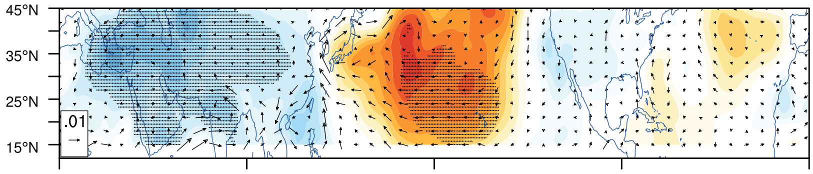

(c) Weak SWI years composite

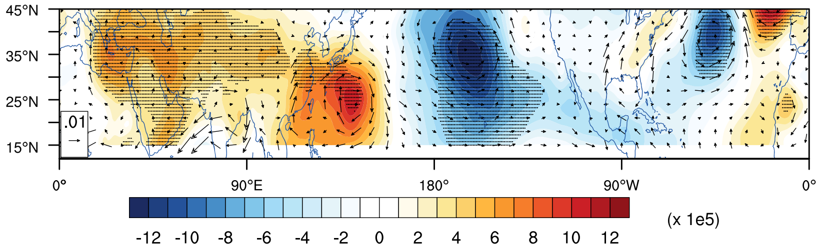

Figure 2. Eddy stream function (shading, unit: $m^2\ s^{-1}$) at 925 hPa and moisture flux (vectors, unit: $kg\ kg^{-1}\ m\ s^{-1}$) at 850 hPa. (a) Climatology; (b) composite of anomalous eddy stream function and moisture flux based on strong SWI years; (c) same as (b) except for weak SWI years. The climatology of vertical integrated moisture flux divergence (contours) is superimposed on (a), where solid (dashed) contours denote positive (zero and negative) values. Contour interval is $2 \times 10^{-5}\ kg\ m^{-2}\ s^{-1}$. The scale of the vectors is shown in the bottom left. Dotted area denotes that the value of the stream function anomalies is statistically significant ($p < 0.1$).

Space Administration (NASA), the Japanese 55-year reanalysis (JRA-55) (Kobayashi *et al* 2015) and the National Centers for Environmental Prediction and the National Center for Atmospheric Research (NCEP/NCAR) reanalysis (Kalnay *et al* 1996). The SWI in each dataset shows an upward trend between 1979 and 2013 (figure 1(e)). The Mann–Kendall test indicates that the statistical significance level of the SWI trend is $p < 0.01$ for MERRA, $p < 0.16$ for JRA-55 and $p < 0.25$ for NCEP/NCAR. The correlation coefficients between the SWI for ERA-interim and the SWI for the other three datasets are very high, 0.92 for MERRA, 0.95 for JRA-55 and 0.87 for NCEP/NCAR. These results suggest the amplification of low-level subtropical stationary waves in the boreal summer is a robust signal over recent decades.

To further examine whether the SWI can capture the change in hemispheric stationary wave amplitude, we composite the stream function based on strong and weak SWI years, respectively. The climatology of the stream function at 925 hPa is shown in figure 2(a), while figures 2(b) and (c) demonstrate the anomalous stream function based on strong and weak SWI years, respectively. The strong (weak) SWI years are linked to enhanced (reduced) NPSH and NASH, as well as a deepened (weakened) Eurasian low. These results suggest that the SWI indeed captures the overall amplitude changes of subtropical stationary waves. The positive trend of the SWI indicates an amplification of the stationary waves from 1979 to 2013.

3.2. Changes in moisture flux associated with the wave amplification

In order to understand the impact of amplified stationary waves on precipitation, we investigate corresponding changes in the large-scale water vapor transport using the moisture flux. Since the atmospheric water vapor content decreases rapidly with height, the moisture flux in the lower atmosphere closely resembles the vertically integrated total moisture flux (Schmitz and Mullen 1996, Zhou and Yu 2005). Therefore, we adopt the moisture flux at 850 hPa to represent the water vapor advection associated with the low-level circulation. The climatology of the moisture flux (figure 2(a)) matches that of the stream function very well. The main features of the climatological moisture flux are strong eastward flux over South Asia along the southern edge of the Eurasia Low, northward flux over the western Pacific between the Eurasia Low and the NPSH, and northward moisture flux from the Gulf of Mexico toward North America along the western edge of the NASH, which is largely related to moisture transport by the Great Plains low-level jet (GPLLJ) (Higgins *et al* 1997, Weaver and Nigam 2008). Composites of moisture flux anomalies are superimposed on the stream function

(a) Difference of moisture flux divergence

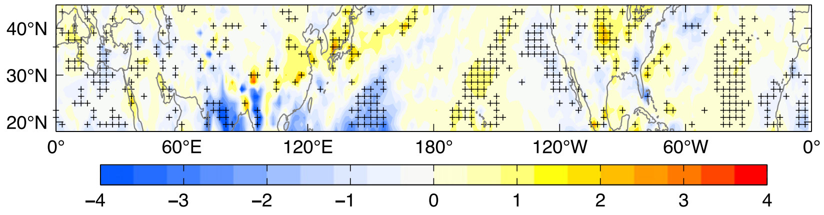

(b) Difference of precipitation

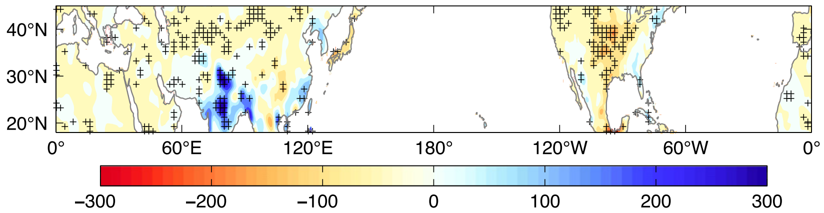

Figure 3. (a) Vertical integral of moisture divergence composite based on strong SWI years minus that based on weak SWI years (shading). Cool colors denote moisture flux convergence, and warm colors denote divergence (Units: 10^{-5} kg m^{-2} s^{-1}). (b) Same as (a) except for seasonal precipitation. The warm colors denote dry anomaly and cool colors wet anomaly (unit: mm). The hatched areas represent where the values are statistically significant ($p < 0.1$).

anomaly in figures 2(b) and (c). In strong SWI years, accompanying the enhanced Eurasia Low, moisture flux from the Indian Ocean toward South Asia and the Indochinese Peninsula is intensified. At the same time, the eastward-extended cyclonic circulation increases moisture flux over the western Pacific. The enhanced NASH in the strong SWI years has a southwest extension, which induces intensified moisture flux toward the southeast United States and weakened GPLLJ. In contrast, the weak SWI years are related to the weakened moisture flux over South Asia and the Indochinese Peninsula. Coinciding with the contraction of the NPSH and the weakening of the Eurasia low, an anti-cyclonic circulation is observed over the western Pacific, which decreases the moisture flux over the western Pacific and increases the moisture flux over East Asia. Over the Western Hemisphere, the climatology of vertical motion associated with the NASH is upward over the western portion and downward over the eastern portion of the NASH (Rodwell and Hoskins 2001, Miyasaka and Nakamura 2005). The weakened NASH decreases the rising motion over its western portion (not shown), associated with anomalous high in the lower troposphere over the eastern United States, which enhances the GPLLJ and brings increased moisture flux to the central United States. We further examine the vertical integral of the moisture flux divergence, which is commonly used to estimate precipitation in weather forecasting (Banacos and Schultz 2005). The climatology of the moisture flux divergence (figure 2(a)) exhibits convergence over western oceans and eastern continents, as well as divergence over eastern oceans and western continents. Figure 3(a) shows the moisture flux divergence composite based on strong SWI years minus that based on weak SWI years, which enables a comparison between the large and small amplitude of subtropical stationary waves. This suggests that the amplified subtropical stationary waves are related to intensified convergence of moisture flux over South Asia, the western Indochinese Peninsula, the western North Pacific and the eastern United States; as well as intensified divergence over northern China, the northwestern and central North Pacific, central United States and the eastern North Atlantic. These features are closely consistent with the moisture flux anomalies (figure 2), indicating that the water vapor divergence/convergence in these regions is related to the water vapor transport by the large-scale flow. The fact that changes in moisture flux coincide with the stream function anomalies suggests that the stationary wave amplification has a strong potential to impact regional precipitation.

3.3. Relationships between subtropical stationary waves and regional water extremes

In section 3.2, we found that boreal summer subtropical stationary waves have amplified during recent decades and that corresponding changes in lower tropospheric circulation modify moisture transport. Whether these changes contribute to the seasonal precipitation amount and the occurrence of regional water extremes (i.e., droughts and heavy rainfall events) is investigated in this section.

First we examine the relationship between subtropical stationary waves and the total precipitation amount in JJA. Figure 3(b) shows the precipitation difference between strong and weak SWI years. When the stationary waves are amplified, there is more precipitation over South Asia, southeastern China and the eastern United States, but less precipitation over northern China, Japan, the central United States and Mexico.

(a) Difference of dry day number

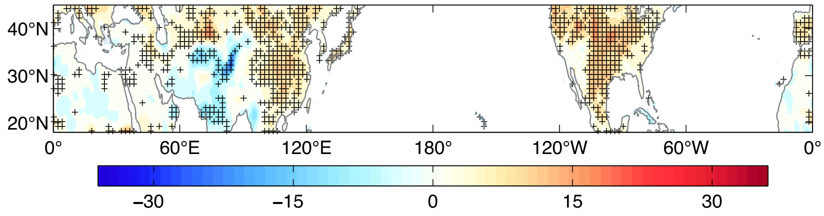

(b) Difference of heavy-rainfall day number

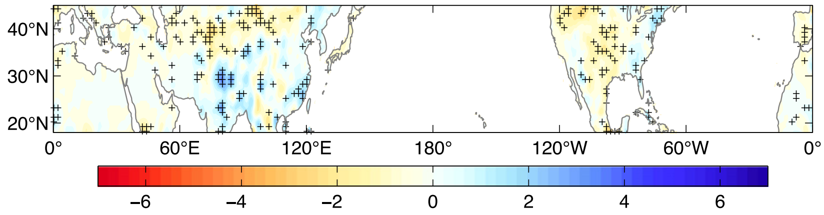

Figure 4. (a) Numbers of dry days composite based on strong SWI years minus that based on weak SWI years. Warm colors denote increased dry days, and cool colors decreased dry days. (b) Same as (a) but for heavy-rainfall days. Cool colors denote increased wet days, and warm colors decreased wet days (units: days). The hatched areas represent where the values are statistically significant ($p < 0.1$).

These results are similar to those obtained by the NOAA's Precipitation Reconstruction over Land (PREC/L) (Chen *et al* 2002) dataset (not shown). Over the continents, the pattern of precipitation difference resembles the pattern of moisture flux divergence difference (figure 3(a)): the area of increased (decreased) precipitation coincides with the area of moisture flux convergence (divergence) anomalies. The pattern correlation between the difference of precipitation (figure 3(b)) and the difference of moisture flux divergence (figure 3(a)) is -0.5 (statistically significant at $p < 0.05$). This indicates that the amplification of stationary waves might contribute to changes in seasonal precipitation by modifying the moisture transport through large-scale circulation.

To further investigate the influence on water extremes, we composite the numbers of dry and heavy-rainfall days based on strong and weak SWI years, separately. Figures 4(a) and (b) show the composite of extreme-day numbers based on strong SWI years minus that based on weak SWI years for dry days and for heavy-rainfall days, respectively. The distributions of changes in the probability of both dry days and heavy-rainfall days are consistent with the distribution of changes in precipitation. The pattern correlation is -0.4 between the difference of precipitation (figure 3(b)) and the difference of dry-day numbers (figure 4(a)), and 0.76 between the difference of precipitation (figure 3(b)) and the difference of heavy-rainfall day numbers (figure 4(b)). Both pattern correlation coefficients are statistically significant ($p < 0.05$). Amplified stationary waves are associated with increased frequency of dry days (thus a higher chance of drought occurrence) over eastern and northwestern China, Japan, central and northwestern United States, and Mexico (figure 4(a)), where the seasonal precipitation is also decreased (figure 3(b)). At the same time, we can observe increased frequency of heavy-rainfall days over South Asia, some locations over southeastern China, and the eastern United States (figure 4(b)), where the seasonal precipitation is increased (figure 3(b)). These results suggest that changes in the probability of water extremes likely share a similar physical mechanism to changes in seasonal precipitation through the variation in moisture transport associated with the amplification of subtropical stationary waves.

4. Discussion

Previous studies primarily investigated the impact of subtropical circulation (e.g. subtropical highs and monsoons) on precipitation on a regional basis (Higgins and Shi 2000, Wang *et al* 2001, Li *et al* 2011). They revealed indigenous features resulting from regional circulation patterns. Some recent studies (Hsu *et al* 2011, Wang *et al* 2012, 2013) on monsoon variability and change have demonstrated that the response of circulation to the warming climate usually takes place beyond the regional scale, yet they primarily focus on monsoon precipitation. Therefore, we investigate subtropical stationary waves to identify coherent changes and overriding impacts on a *hemispheric* scale. Our results illustrate a close relationship between the amplified subtropical stationary waves and variations in the hydro climate and show that this relationship is established through large-scale moisture transport by wave flows. The combined effects of monsoon lows and subtropical highs reveal features that are not easily identified and explained through regional approaches. Furthermore, this study elucidates the types and locations of water extremes associated with the amplification of stationary waves in the subtropics. These details could provide important guidance for policy makers in evaluating the risk of water extremes and deciding on related mitigation/adaptation strategies.

Over recent decades, both observational evidence and model simulations have shown a significant intensification of the land–sea thermal contrast over the NH (Sutton *et al* 2007, Wang *et al* 2012). Over the latitude band 15 °N–45 °N, the land–sea temperature ratio [land-surface air temperature from Climate Research Unit (Jones *et al* 2001) over the sea surface temperature from HadISST1 (Rayner *et al* 2003)] shows a statistically significant ($p < 0.01$) positive trend during JJA from 1979 to 2013 (figure not shown). The increased land–sea temperature difference could largely change the diabatic heating. Since subtropical stationary waves are mainly maintained by diabatic heating (Ting 1994, Miyasaka and Nakamura 2005), the intensified land–sea thermal contrast is likely a mechanism for the amplification of subtropical stationary waves in the boreal summer (Shaw and Voigt 2015). This hypothesis indicates a different clue for the amplification of planetary waves in climate change from the previous studies that primarily link the amplified planetary waves to the Arctic amplification.

Furthermore, this hypothesis may also help us to better understand why the SWI trend is significantly positive near the surface, rather than at the upper level. Since the near-surface diabatic heating associated with the land–sea thermal contrast is an important source for the maintenance of the subtropical highs as well as the planetary waves during the summer (Miyasaka and Nakamura 2005), the response of subtropical stationary waves to the increase in land–sea thermal contrast tends to attain significant amplitude near the surface. In the upper troposphere, the difference between the temperature over land and over the ocean is smaller than that near the surface (Byrne and O'Gorman 2013). The upper-level subtropical stationary waves are maintained by multiple sources, e.g. the upward component of wave activity flux from near-surface forcing (Miyasaka and Nakamura 2005), as well as wave activity injections from the tropics (Hoskins and Karoly 1981) and higher latitudes (Hoskins and Ambrizzi 1993). These indicate that the responses of upper level stationary waves to changes in near-surface diabatic heating are indirect and weaker compared with near surface responses. In summary, the stronger trend of subtropical stationary waves found at lower levels suggests the increased land–sea thermal contrast as a likely forcing mechanism of the trend. The validity of this hypothesis needs to be tested using numerical models.

5. Conclusions

We have diagnosed changes in the subtropical stationary wave amplitude in the boreal summer and investigated their implication for regional water extremes through changing large-scale water vapor transport. The investigation, based on the SWI, suggests an amplification of the subtropical stationary waves in boreal summer from 1979 to 2013. This amplification of the subtropical stationary waves is characterized by an enhancement of the subtropical highs and the Eurasian Low. The corresponding changes in large-scale circulation are related to an intensified South Asian monsoon, and decreased GPLLJ. Accompanying the wave amplification, changes in large-scale moisture flux lead to increased precipitation over South Asia, southeastern China and the eastern United States, as well as decreased precipitation over the central United States, Mexico, Japan and northern China. Consistent with the seasonal precipitation anomaly, the analysis of water extremes suggested an increased dry day (drought) frequency over the northwestern and central United States, Mexico, Japan, and northwestern and eastern China, along with increased heavy-rainfall days over South Asia, southeastern China and the eastern United States. These results indicate that the amplification of stationary waves will be accompanied by anomalous moisture flux convergence/divergence in some regions which could increase the probability of floods or droughts.

Acknowledgements

We would like to thank the ECMWF for providing the ERA-interim data (http://apps.ecmwf.int/datasets/data/interim-full-daily/), and CPC US Unified Precipitation data (http://www.esrl.noaa.gov/psd/). This research is funded by the National Science Foundation Grant AGS-1147608, the National Institutes of Health Grant, NIH-1R21AG044294-01A1; Yi Deng is supported by the National Science Foundation under grants AGS-1147601, AGS-1354402, and AGS-1445956. We also would like to thank Dr Femke De Jong and Patrick Brown for editorial assistance in English.

References

Adams D K and Comrie A C 1997 The North American monsoon *Bull. Am. Meteorol. Soc.* **78** 2197–213

Balk D, Deichmann U and Yetman G 2010 ISLSCP II global population of the world *ISLSCP Initiative II Collection. Data set* ed F G Hall *et al* (doi:10.3334/ORNLDAAC/975)

Banacos P C and Schultz D M 2005 The use of moisture flux convergence in forecasting convective initiation: historical and operational perspectives *Weather Forecast.* **20** 351–66

Barnes E A 2013 Revisiting the evidence linking Arctic amplification to extreme weather in midlatitudes *Geophys. Res. Lett.* **40** 4734–9

Braganza K, Karoly D J, Hirst A C, Stott P, Stouffer R J and Tett S F B 2004 Simple indices of global climate variability and change part II: attribution of climate change during the twentieth century *Clim. Dyn.* **22** 823–38

Byrne M P and O'Gorman P A 2013 Land–ocean warming contrast over a wide range of climates: convective quasi-equilibrium theory and idealized simulations *J. Clim.* **26** 4000–16

Chen M Y, Shi W, Xie P P, Silva V B S, Kousky V E, Higgins R W and Janowiak J E 2008 Assessing objective techniques for gauge-based analyses of global daily precipitation *J. Geophys. Res.—Atmos.* **113** D04110

Chen M Y, Xie P P, Janowiak J E and Arkin P A 2002 Global land precipitation: A 50-yr monthly analysis based on gauge observations *J. Hydrometeorol.* **3** 249–66

Chen S C and Trenberth K E 1988 Forced planetary-waves in the northern hemisphere winter—wave-coupled orographic and thermal forcings *J. Atmos. Sci.* **45** 682–704

Chen T C 2003 Maintenance of summer monsoon circulations: a planetary-scale perspective *J. Clim.* **16** 2022–37

Chen T C 2010 Characteristics of summer stationary waves in the northern hemisphere *J. Clim.* **23** 4489–507

Coumou D, Petoukhov V, Rahmstorf S, Petri S and Schellnhuber H J 2014 Quasi-resonant circulation regimes and hemispheric synchronization of extreme weather in boreal summer *Proc. Natl Acad. Sci. USA* **111** 12331–6

Coumou D and Rahmstorf S 2012 A decade of weather extremes *Nat. Clim. Change* **2** 491–6

Coumou D, Robinson A and Rahmstorf S 2013 Global increase in record-breaking monthly-mean temperatures *Clim. Change* **118** 771–82

Davis R E, Hayden B P, Gay D A, Phillips W L and Jones G V 1997 The north atlantic subtropical anticyclone *J. Clim.* **10** 728–44

Dee D P *et al* 2011 The ERA-Interim reanalysis: configuration and performance of the data assimilation system *Q. J. R. Meteorol. Soc.* **137** 553–97

Dole R, Hoerling M, Perlwitz J, Eischeid J, Pegion P, Zhang T, Quan X, Xu T and Murray D 2011 Was there a basis for anticipating the 2010 Russian heat wave? *Geophys. Res. Lett.* **38** L06702

Francis J A and Vavrus S J 2012 Evidence linking Arctic amplification to extreme weather in mid-latitudes *Geophys. Res. Lett.* **39** L06801

Francis J A and Vavrus S J 2015 Evidence for a wavier jet stream in response to rapid Arctic warming *Environ. Res. Lett.* **10** 014005

Hassanzadeh P, Kuang Z M and Farrell B F 2014 Responses of midlatitude blocks and wave amplitude to changes in the meridional temperature gradient in an idealized dry GCM *Geophys. Res. Lett.* **41** 5223–32

Higgins R W and Shi W 2000 Dominant factors responsible for interannual variability of the summer monsoon in the southwestern United States *J. Clim.* **13** 759–76

Higgins R W, Yao Y, Yarosh E S, Janowiak J E and Mo K C 1997 Influence of the great plains low-level jet on summertime precipitation and moisture transport over the central United States *J. Clim.* **10** 481–507

Holloway C E and Neelin J D 2009 Moisture vertical structure, column water vapor, and tropical deep convection *J. Atmos. Sci.* **66** 1665–83

Holton J R 1992 *Introduction to Dynamic Meteorology* 3rd edn (New York: Academic) pp 379–80

Hoskins B J and Ambrizzi T 1993 Rossby wave propagation on a realistic longitudinally varying flow *J. Atmos. Sci.* **50** 1661–71

Hoskins B J and Karoly D J 1981 The steady linear response of a spherical atmosphere to thermal and orographic forcing *J. Atmos. Sci.* **38** 1179–96

Hsu P, Li T and Wang B 2011 Trends in global monsoon area and precipitation over the past 30 years *Geophys. Res. Lett.* **38** L08701

Jones P D, Osborn T J, Briffa K R, Folland C K, Horton E B, Alexander L V, Parker D E and Rayner N A 2001 Adjusting for sampling density in grid box land and ocean surface temperature time series *J. Geophys. Res.* **106** 3371–80

Kalnay E *et al* 1996 The NCEP/NCAR 40-year reanalysis project *Bull Am. Meteorol. Soc.* **77** 437–70

Kamae Y, Watanabe M, Kimoto M and Shiogama H 2014 Summertime land–sea thermal contrast and atmospheric circulation over east asia in a warming climate: I. Past changes and future projections *Clim. Dyn.* **43** 2553–68

Kobayashi S *et al* 2015 The JRA-55 reanalysis: general specifications and basic characteristics *J. Meteor. Soc. Japan, Ser. II* **93** 5–48

Li W, Li L, Fu R, Deng Y and Wang H 2011 Changes to the North Atlantic subtropical high and its role in the intensification of summer rainfall variability in the Southeastern United States *J. Clim.* **24** 1499–506

Li W, Li L, Ting M F, Deng Y, Kushnir Y, Liu Y, Lu Y, Wang C and Zhang P 2013 Intensification of the Southern Hemisphere summertime subtropical anticyclones in a warming climate *Geophys. Res. Lett.* **40** 5959–64

Li W, Li L, Ting M F and Liu Y M 2012 Intensification of northern hemisphere subtropical highs in a warming climate *Nat. Geosci.* **5** 830–4

Liu J, Curry J A, Wang H, Song M and Horton R M 2012 Impact of declining Arctic sea ice on winter snowfall *Proc. Natl Acad. Sci. USA* **109** 4074–9

Min S K, Zhang X, Zwiers F W and Hegerl G C 2011 Human contribution to more-intense precipitation extremes *Nature* **470** 378–81

Miyasaka T and Nakamura H 2005 Structure and formation mechanisms of the northern hemisphere summertime subtropical highs *J. Clim.* **18** 5046–65

Nigam S and DeWeaver E 2003 Stationary waves (orographic and thermally forced) *Encyclopedia of Atmospheric Sciences* ed J R Holton *et al* (London: Academic) pp 2243–69

Pall P, Aina T, Stone D A, Stott P A, Nozawa T, Hilberts A G J, Lohmann D and Allen M R 2011 Anthropogenic greenhouse gas contribution to flood risk in England and Wales in autumn 2000 *Nature* **470** 382–5

Petoukhov V, Rahmstorf S, Petri S and Schellnhuber H J 2013 Quasiresonant amplification of planetary waves and recent northern hemisphere weather extremes *Proc. Natl Acad. Sci. USA* **110** 5336–41

Rahmstorf S and Coumou D 2011 Increase of extreme events in a warming world *Proc. Natl Acad. Sci. USA* **108** 17905–9

Rayner N A, Parker D E, Horton E B, Folland C K, Alexander L V, Rowell D P, Kent E C and Kaplan A 2003 Global analyses of sea surface temperature, sea ice and night marine air temperature since the late nineteenth century *J. Geophys. Res.* **108** 4407

Rienecker M M *et al* 2011 MERRA: NASA's modern-era retrospective analysis for research and applications *J. Clim.* **24** 3624–48

Rodwell M J and Hoskins B J 2001 Subtropical anticyclones and summer monsoons *J. Clim.* **14** 3192–211

Schmitz J T and Mullen S L 1996 Water vapor transport associated with the summertime north american monsoon as depicted by ECMWF analyses *J. Clim.* **9** 1621–34

Screen J A and Simmonds I 2010 The central role of diminishing sea ice in recent Arctic temperature amplification *Nature* **464** 1334–7

Screen J A and Simmonds I 2013 Exploring links between Arctic amplification and mid-latitude weather *Geophys. Res. Lett.* **40** 959–64

Screen J A and Simmonds I 2014 Amplified mid-latitude planetary waves favour particular regional weather extremes *Nat. Clim. Change* **4** 704–9

Shaw T A and Voigt A 2015 Tug of war on summertime circulation between radiative forcing and sea surface warming *Nat. Geosci.* **8** 560–6

Sui C H, Chung P-H and Li T 2007 Interannual and interdecadal variability of the summertime western north pacific subtropical high *Geophys. Res. Lett.* **34** L11701

Sutton R T, Dong B and Gregory J M 2007 Land/sea warming ratio in response to climate change: IPCC AR4 model results and comparison with observations *Geophys. Res. Lett.* **34** L02701

Tang Q H, Zhang X J and Francis J A 2014 Extreme summer weather in northern mid-latitudes linked to a vanishing cryosphere *Nat. Clim. Change* **4** 45–50

Ting M F 1994 Maintenance of northern summer stationary waves in a Gcm *J. Atmos. Sci.* **51** 3286–308

Wang B, Liu J, Kim H J, Webster P J and Yim S Y 2012 Recent change of the global monsoon precipitation (1979-2008) *Clim. Dyn.* **39** 1123–35

Wang B, Liu J, Kim H J, Webster P J, Yim S Y and Xiang B Q 2013 Northern hemisphere summer monsoon intensified by mega-El Nino/southern oscillation and Atlantic multidecadal oscillation *Proc. Natl Acad. Sci. USA* **110** 5347–52

Wang B, Wu R and Lau K-M 2001 Interannual variability of the asian summer monsoon: contrasts between the indian and the western north pacific–east asian monsoons *J. Clim.* **14** 4073–90

Weaver S J and Nigam S 2008 Variability of the great plains low-level jet: large-scale circulation context and hydroclimate impacts *J. Clim.* **21** 1532–51

White G H 1982 An Observational Study of the Northern Hemisphere Extratropical Summertime General-Circulation *J. Atmos. Sci.* **39** 24–40

Woollings T, Harvey B and Masato G 2014 Arctic warming, atmospheric blocking and cold European winters in CMIP5 models *Environ. Res. Lett.* **9** 014002

Zhou T *et al* 2009 Why the western pacific subtropical high has extended westward since the late 1970s *J. Clim.* **22** 2199–215

Zhou T and Yu R 2005 Atmospheric water vapor transport associated with typical anomalous summer rainfall patterns in China *J. Geophys. Res.* **110** D08104